Research Article Vol. 24, No. 15 | 25 Jul 2016 | OPTICS EXPRESS 17303
Optics EXPRESS

Spectrally resolved white light interferometry to measure material dispersion over a wide spectral band in a single acquisition

YAGO AROSA, ELENA LÓPEZ LAGO, LUIS MIGUEL VARELA, RAÚL DE LA FUENTE*

Grupo de Nanomateriais, Fotónica e Materia Branda, Departamentos de Física Aplicada e de Física da Materia Condensada, Universidade de Santiago de Compostela, E-15782, Santiago de Compostela, Spain
* *raul.delafuente@usc.es*

Abstract: In this paper we apply spectrally resolved white light interferometry to measure refractive and group index over a wide spectral band from 400 to 1000 nm. The output of a Michelson interferometer is spectrally decomposed by a homemade prism spectrometer with a high resolution camera. The group index is determined directly from the phase extracted from the spectral interferogram while the refractive index is estimated once its value at a given wavelength is known

©2016 Optical Society of America

OCIS codes: (120.0120) Instrumentation, measurement, and metrology; (120.2650) Fringe analysis; (120.3180) Interferometry; (120.5050) Phase measurement; (290.3030) Index measurements.

References and links

1. L. M. Smith and C. C. Dobson, “Absolute displacement measurements using modulation of the spectrum of white light in a Michelson interferometer,” Appl. Opt. **28**(16), 3339–3342 (1989).
2. P. Hlubina, “Dispersive white-light spectral interferometry to measure distances and displacements,” Opt. Commun. **21**(1-3), 65–70 (2002).
3. C. Sáinz, P. Jourdain, R. Escalona, and J. Calatroni, “Real time interferometric measurements of dispersion curves,” Opt. Commun. **111**(5-6), 632–641 (1994).
4. P. Hlubina, D. Ciprian, and L. Knyblová, “Direct measurement of dispersion of the group refractive indices of quartz crystal by white-light spectral interferometry,” Opt. Commun. **269**(1), 8–13 (2007).
5. J. Calatroni, A. L. Guerrero, C. Sáinz, and R. Escalona, “Spectrally-resolved white-light interferometry as a profilometry tool,” Opt. Laser Technol. **28**(7), 485–489 (1996).
6. S. K. Debnath, M. P. Kothiyal, J. Schmit, and P. Hariharan, “Spectrally resolved phase-shifting interferometry of transparent thin films: sensitivity of thickness measurements,” Appl. Opt. **45**(34), 8636–8640 (2006).
7. H.-T. Shang, “Chromatic dispersion measurement by white-light interferometry on metre-length single-mode optical fibres,” Electron. Lett. **17**(17), 603–605 (1981).
8. J. Y. Lee and D. Y. Kim, “Versatile chromatic dispersion measurement of a single mode fiber using spectral white light interferometry,” Opt. Express **14**(24), 11608–11615 (2006).
9. R. C. Youngquist, S. M. Simmons, and A. M. Belanger, “Spectrometer wavelength calibration using spectrally resolved white-light interferometry,” Opt. Lett. **35**(13), 2257–2259 (2010).
10. R. de la Fuente, “White light spectral interferometry as a spectrometer calibration tool,” Appl. Spectrosc. **68**(5), 525–530 (2014).
11. J. Tapia-Mercado, A. V. Khomenko, and A. Garcia-Weidner, “Precision and sensitivity optimization for white-light interferometric fiber-optic sensors,” J. Lightwave Technol. **19**(1), 70–74 (2001).
12. S. P. Ng, C. M. L. Wu, S. Y. Wu, and H. P. Ho, “White-light spectral interferometry for surface plasmon resonance sensing applications,” Opt. Express **19**(5), 4521–4527 (2011).
13. P. Hlubina, “White-light spectral interferometry with the uncompensated Michelson interferometer and the group refractive index dispersion in fused silica,” Opt. Commun. **193**(1-6), 1–7 (2001).
14. H. Delbarre, C. Przygodzki, M. Tassou, and D. Boucher, “High-precision index measurement in anisotropic crystals using white-light spectral interferometry,” Appl. Phys. B **70**(1), 45–51 (2000).
15. D. Reolon, M. Jacquot, I. Verrier, G. Brun, and C. Veillas, “High resolution group refractive index measurement by broadband supercontinuum interferometry and wavelet-transform analysis,” Opt. Express **14**(26), 12744–12750 (2006).
16. Kramida, A., Ralchenko, Yu., Reader, J. and NIST ASD Team (2015). NIST Atomic Spectra Database (version 5.3), [Online]. Available: http://physics.nist.gov/asd (accesed Apr. 27 2016). National Institute of Standards and Technology, Gaithersburg, MD.

#267722 http://dx.doi.org/10.1364/OE.24.017303
Journal © 2016 Received 3 Jun 2016; revised 13 Jul 2016; accepted 13 Jul 2016; published 21 Jul 2016

17. C. Sáinz, P. Jourdain, R. Escalona, and J. Calatroni, "Real time interferometric measurements of dispersion curves," Opt. Commun. **111**(5-6), 632–641 (1994).
18. D. X. Hammer, A. J. Welch, G. D. Noojin, R. J. Thomas, D. J. Stolarski, and B. A. Rockwell, "Spectrally resolved white-light interferometry for measurement of ocular dispersion," J. Opt. Soc. Am. A **16**(9), 2092–2102 (1999).
19. M. N. Polyanskiy, "Refractive index database," http://refractiveindex.info (accessed Apr. 26 2016)

1. Introduction

Spectrally resolved white light interferometry (SRWLI) or white light spectral interferometry is a well-known interferometric technique that uses an incoherent light source to illuminate an interferometer followed by a spectrometer that resolves the interferogram at each wavelength. SRWLI is applied to measure distances, thicknesses or displacements [1,2] and material dispersion [3,4]; it is used in optical profilometry [5,6], broadband optical communication applications [7,8], spectrometer calibration [9,10] or as a light sensor [11,12].

Although this technique is denominated "white light", the spectra of the source can expand from a few nanometers to hundreds of nanometers in the UV, VIS or IR band. For example, to measure displacements or distances over a range of some millimeters we must use a high resolution spectrometer with a narrow spectral band, while to measure displacements with high accuracy (below one micron) we must use a broadband spectrometer. On the other hand, the characterization of materials demands the usage of a spectral band as wide as possible, while preserving high resolution, a challenge that must be properly undertaken. This can be made in two ways, by resolving a series of narrow spectrograms to determine dispersion sequentially at different wavelengths or by resolving a single (or few) spectrogram to determine dispersion in a broad band. For example, Hlubina [13] used a low resolution spectrometer to obtain group index over 450 to 900 nm by sequentially evaluating the stationary phase point position as a function of the interferometer path length difference in air; Delbarre et al. [14] processed three interferograms including a stationary phase point to get the group index and estimated the refractive index from 540 to 660 nm; Reolon et al. [15] used a broadband supercontinuum source with high degree of spatial coherence to increase the fringe visibility and measured group index from 530 to 800 nm in a single acquisition. The challenge to determine dispersion in a single acquisition over a wide spectral band is that the sample induces a varying frequency chirp in the wave-number domain that increases as we move away from the stationary phase point, and hence diminishes fringe visibility at the borders of the spectra. Though, a broadband spectrometer is needed with enough resolution to resolve high frequency fringes over the desired spectral range, especially for thick samples and strongly dispersive materials.

In our case, we are interested in determining material dispersion in the VIS_NIR band (400 - 1000 nm). Typically, commercial grating spectrometers used in WRLSI experiments do not resolve the fringes in this wide spectral window. So, we assembled a prism spectrometer with a high resolution camera to increase the visibility function. The difference between a grating and a prism spectrometer is the way of separating the spectra. In the former, dispersion is nearly linear in wavelength, while the latter is highly nonlinear in wavelength but more linear in wavenumber ($\sigma = 1/\lambda$, in air). In Fig. 1, we show the simulation of two ideal white light spectral interferograms (with visibility one and constant irradiance) corresponding to the dispersion in a fused silica sample as they are seen in a typical grating spectrometer and in our home made prism spectrometer. In the case of the grating spectrometer, we used the measured dispersion of a commercial miniature spectrometer to simulate the interferogram; furthermore, in both cases we consider a 3648 pixels linear camera, spanning the spectra from 400 to 1000 nm. We see that the frequency chirp is above three times greater at the border of the spectra for the grating spectrometer. In a real case, the finite spectrometer resolution will deteriorate the fringe visibility and will decrease further the possibility of resolving the interferogram. Furthermore, prism

Optics EXPRESS

spectrometers present greater dispersion power for high frequencies in the visible band, where the material dispersion is typically greater, and consequently the refractive index variation, and lower dispersion for the IR band where the refractive index varies slowly.

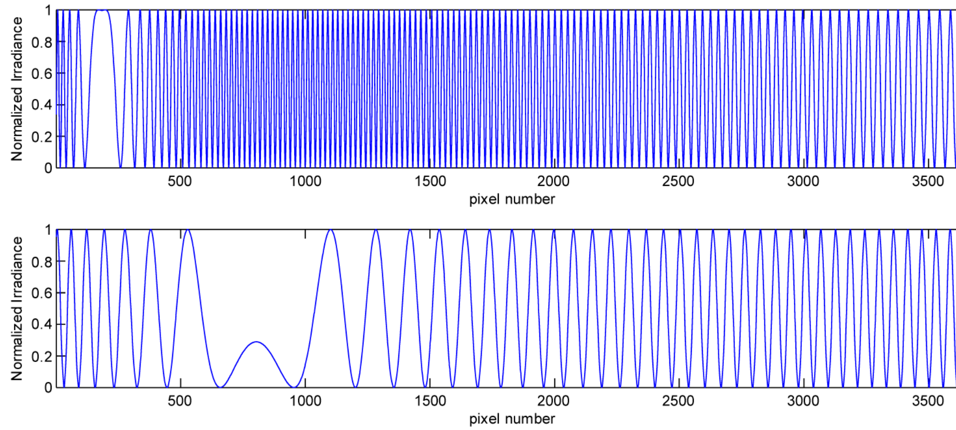

Fig. 1. Simulation of ideal interferograms, with constant background irradiance and visibility of one, for a typical grating spectrometer (a) and for our home-made prism spectrometer (b) when we insert in one of the arms of the interferometer a silica plate 1 mm thick. In the former case we used the calibration of a commercial portable spectrometer and in the second case we used the calibration discussed in section 2.

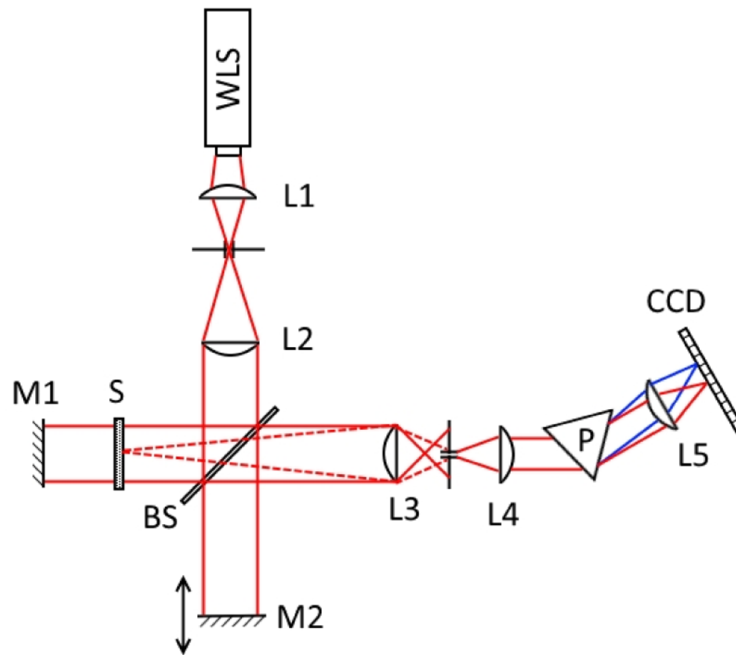

Fig. 2. Experimental setup; WLS white light source; L1 - L4 lenses; M1 fixed mirror; M2 moving mirror; BS beam splitter; S sample; P prism

In the next sections, we present dispersion measurements for three different optical glasses (fused silica, BK7 and D263t Schott glass) over a wide spectral band from 400 to 1000 nm in a single acquisition. The group index is directly obtained from phase processing

Optics EXPRESS

of the spectral interferogram, while refractive index measurement is estimated with high accuracy by knowing its value at a given wavelength.

2. Experimental set-up

In Fig. 2 we show the experimental configuration. SRWLI measurements were taken with a 135 W halogen lamp which illuminates a standard Michelson interferometer with no specific characteristics other than being transparent in the spectral range of the spectrometer. As usual, one of the interferometer mirrors can be adjusted to superimpose precisely the two beams that travel along the interferometer arms, and the other mirror can be translated to vary the optical pathlength in its own arm. The output of the interforometer is spectrally separated by an F2 equilateral dispersive prism in a 315 mm focal length spectrometer, and imaged on a high resolution linear camera with 3648 pixels 8 x 200 μm^2 wide. The prism was oriented so that the camera sensor spans a broadband spectral band from 390 to 1045 nm, approximately. In contrast with a grating spectrometer in which the relationship between wavelength and pixel number is mainly linear, with a small non-linear contribution, a prism spectrometer is highly non-linear in wavelength, with lower blue-green wavelength highly dispersed in comparison to red-IR wavelength, as it is seen in Fig. 3(a).

We paid special attention to the calibration of the experimental apparatus, an issue often overlooked but that is essential to get high precision values of refractive and group indexes. The spectrometer was calibrated with an Hg-Ar lamp; the different peaks shown in Fig. 3(a) were used to perform the calibration by fitting those to a fourth order polynomial in σ. In Fig. 3(b) it is shown the fit as a function of wavenumber and wavelength. The fit in wavelength was obtained directly from the curve in wavenumber by inversion, because we were not able to perform a polynomial fit since it fails at small wavelengths at the right side of the first Hg-Ar line. In Fig. 3(c) it is plotted the spectral bandpass of each pixel showing higher dispersion at the blue wavelengths. The bandpass (in wavelength units) goes from 0.04 nm at the blue end of the spectra to 0.8 nm at the IR end, enough to resolve for dispersion in typical materials, even strong dispersive ones.

Optics EXPRESS

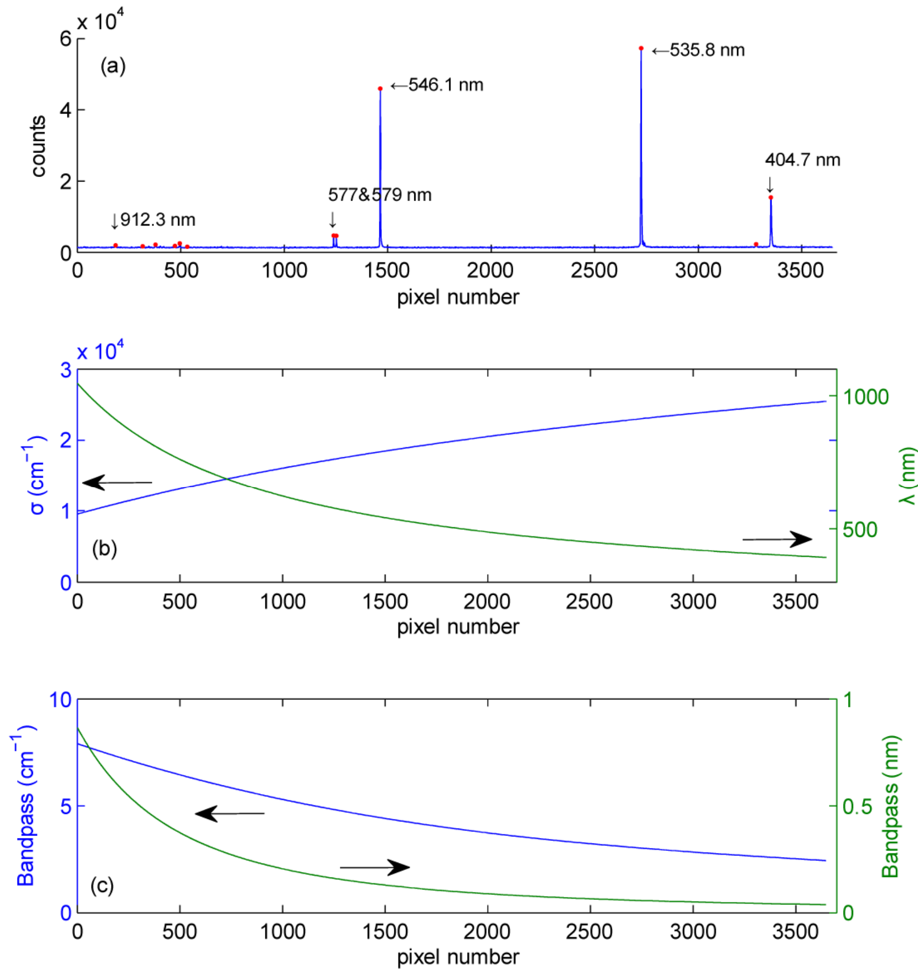

Fig. 3. Calibration of the spectrometer. (a) Image of the lines of Hg-Ar lamp, showing (red dots) the lines used for calibration; (b) Fit of wavenumber (left) and wavelength (right) versus pixel number; (c) bandpass of each pixel.

When a sample with refractive index $n(\sigma)$ and thickness d is disposed in one of the arms of the interferometer, the spectral irradiance at the camera sensor for a given path difference in air l can be written as:

$$I(\sigma) = I_0(\sigma)\left[1 + V(\sigma)\cos\varphi(\sigma)\right] \tag{1}$$

where $I_0(\sigma)$ is the background spectral irradiance, $V(\sigma)$ is the fringe visibility and $\varphi(\sigma)$ the phase:

$$\varphi(\sigma) = 4\pi\sigma\left[d\left(n - n_{air}\right) - n_{air}l\right] \tag{2}$$

Optics EXPRESS

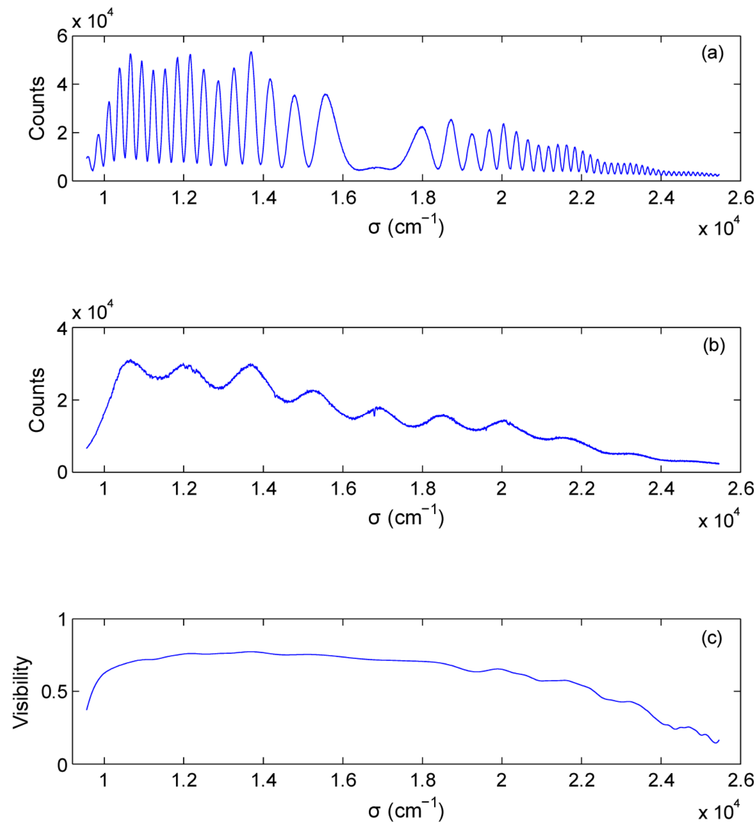

Fig. 4. Typical spectral interferogram obtained with a BK7 plate 2 mm thick. (a) Total signal for a path difference l = 0.55 mm; (b) the background signal; (c) the visibility function.

In Fig. 4 we show the total signal measured by the linear sensor, the background signal and visibility function for a BK7 sample with thickness d = 1.0278 ± 0.0005 mm placed in one of the arms of the interferometer with path difference $l = 555 \pm 1$ µm.

The background irradiance at the camera sensor can be obtained directly by changing the path difference up to a distance in which the spectrometer cannot resolve the fringes. Alternatively, it can be obtained from the total irradiance by calculating it upper envelope I_{up} and lower envelope I_{lo} as $\left(I_{lo}+I_{up}\right)/2$. In turn, these can be calculated by interpolation of maxima and minima of the interferogram, after neglecting the stationary phase point. The envelopes are also used to calculate the visibility function as $V(\sigma)=\left(I_{up}-I_{lo}\right)/\left(2I_0\right)=\left(I_{up}-I_{lo}\right)/\left(I_{lo}+I_{up}\right)$.

In Fig. 4(a) it is shown the stationary phase point occurring at an equalization wavenumber $\sigma_{eq} = 1.68\ 10^4\ \text{cm}^{-1}$ ($\lambda_{eq} = 595.24$ nm). In accordance with the frequency chirp, lower near the equalization wavelength and greater far away, the visibility is lower at the borders of the spectra. This reduction in visibility is enhanced by the sharp decreasing of detector responsivity at IR wavelength as seen in Fig. 4(b). At blue wavelengths the reduction of visibility due to lower background irradiance and strong dispersion is partially compensated by higher dispersion power of the spectrometer in this range, allowing us determining dispersion in a very broad band, as will be shown. Finally, it's worth noting that the irradiance modulations seen in Fig. 4(b) are mainly due to the transmission properties of the beam splitter in the interferometer.

To be sure that the material dispersion is correctly measured, the spectral calibration of the spectrometer must be performed with high accuracy, and the sample thickness d and path length in air l must be measured precisely. The differences between the wavenumbers of the Hg-Ar spectral lines used in the spectrometer calibration (the reference values were taken from ref [16].) and their fitted values after calibration lie below 4 cm^{-1} for all spectral lines with a relative uncertainty below 3 10^{-4}. On the other hand, sample thickness was measured with a high resolution digital micrometer with an accuracy of 0.5 µm. To determine mirror displacement in the moving arm of the Michelson interferometer we calibrate the manual micrometer that performs this displacement. Actually, in order to get higher resolution, the micrometer does not push directly the mirror mount, but it uses a lever, so that the mirror displacement is only a fraction of the micrometer displacement. We also used SRWLI to calibrate the displacement [in this case there was not a sample in the interferometer so d = 0 in Eq. (2)], but since displacements are in the mm range we employed a high resolution (<0.01 nm) commercial grating spectrometer with 40 nm spectral band. The results of calibration are plotted in Fig. 5, leading that the relation between mirror displacement and micrometer scale is not completely linear but has a small quadratic term. The difference between the values measured by WLSRI and the fitted values are about 1 micron. We believe that they are mainly due to a small precession that we observed in one whole turn of the micrometer.

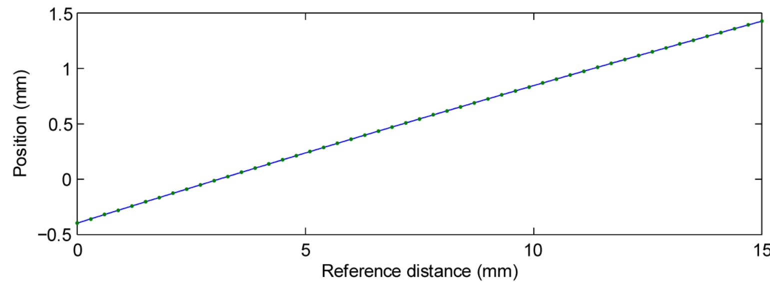

Fig. 5. Calibration of the mirror displacement: measured displacement versus the scale on the manual micrometer.

3. Dispersion measurements

3.1. Group index

The cosine in Eq. (1) can be resolved by retrieving the lower and upper envelopes as explained in the previous section, to obtain:

$$\cos\varphi(\sigma) = 2\frac{I(\sigma) - I_0(\sigma)}{I_{up}(\sigma) - I_{lo}(\sigma)} \tag{3}$$

and the phase can be extracted from the inverse cosine after performing an unwrapping procedure. However, since the cosine function is multivaluated the obtained phase coincides only with the experimental phase in Eq. (2) modulus 2π. That is, the unwrapped phase $\varphi_u(\sigma)$ differs from the experimental phase $\varphi(\sigma)$ by $2k\pi$, $\varphi_u(\sigma) = \varphi(\sigma) - 2k\pi$, with k an unknown integer. Nevertheless, by deriving the phase with respect to σ, we retrieve the group index as:

$$n_g = \frac{d}{d\sigma}(n\sigma) = \frac{1}{4\pi d}\frac{d\varphi_u}{d\sigma} - \left(1 + \frac{l}{d}\right)\frac{d}{d\sigma}(n_{air}\sigma) \tag{4}$$

In practice, to apply Eq. (4) we must choose a suitable path difference in air l to image the spectral interferogram. Indeed, the interferogram can be resolved from a large range of path difference, but visibility is greater when the interferogram includes the phase stationary point. We choose l so that the fringe periodicities in the borders of the spectra are approximately equal. This typically occurs when the stationary phase point is on the green spectrum.

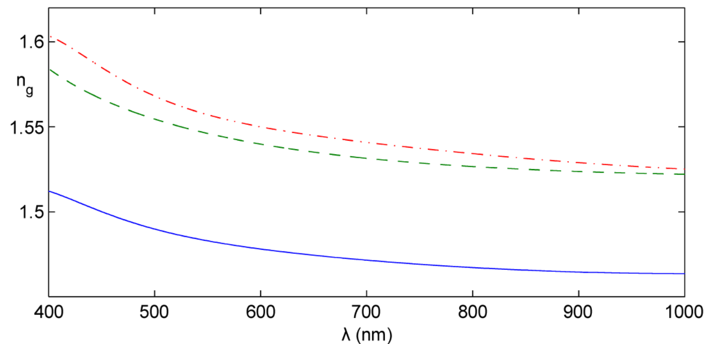

Fig. 6. Group index retrieved directly from phase derivative for a fused silica sample 1mm thick (continuous line), a BK7 sample 2 mm thick (dashed line) and D293T glass sample 210 µm thick (dashed-dotted line) .

The phase retrieved from the spectral interferogram is affected by experimental noise and then the group index obtained by Eq. (4) will be noisy too. To reduce this noise the phase or the calculated group index can be smoothed. Similar results are obtained and we chose to fit to the group index to a polynomial (typically, a fit of order 4th or 5th is sufficient). Results are presented in Fig. 6 for three different optical glasses. The accuracy is below 5 10^{-4} for fused silica and BK7 (except at some wavelengths at the spectra ends). However, for D263t Schott glass the accuracy is worsened over one order of magnitude. We believe that is due to the smaller thickness of the sample and hence smaller path difference in air. The smaller values for these two magnitudes lead to an increase of their relative uncertainties, and consequently to a worse index group retrieval.

3.2. Refractive index

Some authors tried to overcome the $2k\pi$ ambiguity in phase retrieval by fitting to a dispersion relation [17,18], while other authors perfom first the fitting in the phase derivative and then proceed to fit the cosine in Eq. (3) [14]. However, for samples with thickness of hundred of microns or milimeters the k value can be several hundreds or thousands. So, an error in k of one unity can lead to errors in refractive index of 10^{-4} or even 10^{-3}. This can be overcome by selecting thinner samples of tenth of microns when an error in k of one unity leads to errors in refractive index of 10^{-2}, easily detectable.

Other way to resolve this ambiguity consists in measuring separately the refractive index for a given wavelength in order to calculate the k factor directly from the unwraped phase and Eq. (2).

However experimental uncertainty in phase as small as 10^{-3} can lead to appreciable refractive index uncertainty. In this case more data processing is needed. In our case we followed a procedure inspired in [14].

Firstly we assume that the refractive index verifies a Sellmeier dispersion formula with only one resonance, that is:

$$n(\sigma) = \sqrt{A + \frac{B}{1 - C\sigma^2}} \tag{5}$$

and calculate the group index formula for this relation. Then, we determine group index directly from the phase derivative and fit it to the group index dispersion formula to get the values of A, B and C. A first estimation of refractive index is obtained from this value. However, the addition of some function of the type D/σ to the refractive index gives the same group index, so we have an ambiguity in the refractive index. In fact, this ambiguity is similar to the phase ambiguity in the factor $2k\pi$, which means and index ambiguity of $2k\pi/\sigma$. To resolve this ambiguity we use the known refractive index n_0 at a given wavenumber σ_0 to calculate its difference from the estimated refractive index $n(\sigma_0)$ as

$$n(\sigma_0) - n_0 = \frac{D}{\sigma_0} \tag{6}$$

This gives a new estimation of refractive index as

$$n(\sigma) = \sqrt{A + \frac{B}{1 - C\sigma^2}} - \frac{D}{\sigma} \tag{7}$$

In a second step, we replace this formula in Eqs. (2) and (3) and refine the values of the A - D parameters by fitting the cosine of the phase by means of a Levenberg-Marquardt procedure. Now, we take these values to obtain the new refractive index which is used to calculate an average value for k in a broadband region (which can be smaller than the whole spectral band). With this value of k we can obtain the phase without ambiguity and simply use Eq. (2) to get the final refractive index.

In Fig. 7 we plot the results for the studied samples. As before, the retrieval is worst for the D263t glass. Compared with the reference indexes obtain from [19] we get uncertainties below 6 10^{-5} for fused silica and BK7 glass, even if in the intermediate steps n_0 is taken with an accuracy of 10^{-4}. Finally, from this refractive index we can determine again the group index giving values in agreement with those obtained by phase derivation.

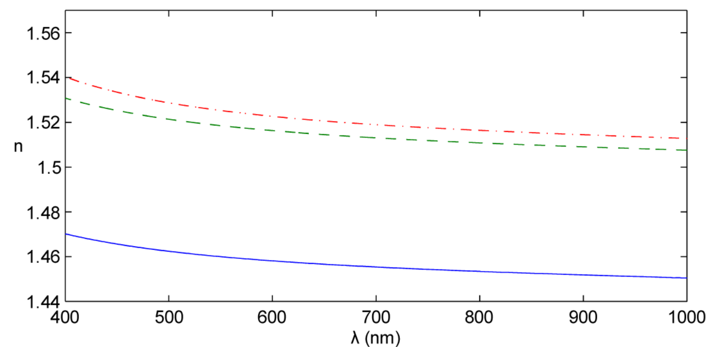

Fig. 7. Retrieved refractive index curve versus wavelength for the same samples as Fig. 6.

4. Conclusions

A prim spectrometer with a high resolution line camera allows characterizing the material dispersion of different samples over a very wide spectral range spanning from 400 to 1000 nm. Such a spectrometer can resolve the interferogram at the output of a Michelson interferometer thus providing the whole experimental data in a single acquisition. The spectral range of characterization can be increased by taking several frames at different bands but this will be limited by the camera sensibility and the range of transparency of the optical elements used in the experimental set-up. Fast measurements over a broad spectral range, including the visible spectrum and more, increase the applicability of the method in many research areas such as design of optical components for imaging instrumentation,

Optics EXPRESS

measurement of ocular dispersions, search of novel liquids for optofluidics, supercontinuum generation, phase matched optical mixing and so on.

The group index was retrieved directly from the derivative of the spectral phase with accuracy about 10^{-4}. While, for retrieving the refractive index we used a known refractive index for a given wavelength to resolve for the phase ambiguity, and after some intermediate steps where the index was assumed to verify some dispersion equations, we finally retrieved the refractive index directly from the phase. The accuracy of the results is below 10^{-4}.

The factors that limit the accuracy are the uncertainty of the path difference in air and the sample thickness. In future works, we will try to improve the measurement of mirror displacement and sample thickness to increase the accuracy in refractive and group index measurements. We also contemplate to integrate in our device a system to measure the refractive index at one wavelength. Finally, the application of this new single-acquisition white light spectral interferometer to molecular and ionic liquids is in progress.

Funding

Ministerio de Economia y Competitividad (MINECO) (MAT2014-57943-C3-1-P, MAT2014-57943-C3-2-P); Xunta de Galicia and FEDER (R2014/015, AGRU 2015/11).

83.47.59.0 {ts '2020-06-01 08:37:44'}